Environmental Science Advances

ROYAL SOCIETY OF CHEMISTRY

PAPER

View Article Online
View Journal | View Issue

Cite this: *Environ. Sci.: Adv.*, 2023, **2**, 1662

Subambient passive radiative cooling effects of barium sulfate and calcium carbonate paints under Malaysia's tropical climate

William Raphael Joseph,[a] Jun Yeang Tan,[a] Apurav Krishna Koyande,[a] Ianatul Khoiroh, *[a] Jerry Joynson[b] and Steve Willis[b]

Global cooling requirements are increasing at an unprecedented rate due to rapid urbanization and population growth, further aggravating climate concerns. Passive radiative cooling is a unique phenomenon that can be utilized to reduce global cooling, energy consumption and alleviate the urban heat island effect. Paints can act as passive cooling devices that are able to reflect incoming sunlight and emit radiation in the atmospheric window (8–13 μm), where it propagates directly into deep space without any interference. In this work, we have successfully fabricated and tested two different types of cooling paints, consisting of $BaSO_4$ and $CaCO_3$ as their respective pigments under Malaysia's tropical climate. Different types of binders, solvents, and pigment concentrations were tested to obtain the most optimum cooling paint configuration. Field test results proved that both cooling paints were able to achieve remarkable subambient temperatures throughout the entire day, even under direct solar irradiation. The $BaSO_4$ cooling paint was able to achieve subambient temperature reductions of up to −6.1 °C and a mean net cooling power of 71.0 W m^{-2} while the $CaCO_3$ cooling paint achieved a maximum subambient temperature reduction of −6.0 °C and a mean net cooling power of 69.9 W m^{-2}. Both paints were able to significantly outperform commercial white paint on a variety of different surfaces, in terms of cooling performance. The hindering effects of various climate conditions including humidity levels and local wind speeds on the overall cooling performance of both the paints were also investigated.

Received 9th June 2023
Accepted 17th October 2023

DOI: 10.1039/d3va00161j

rsc.li/esadvances

Environmental significance

All materials absorb infrared radiation (IR) across a broad range of wavelengths, and often re-emit IR at other wavelengths. The IR emitted by solid bodies is generally absorbed by the air surrounding the body, such that the air acts as a blanket stopping the body from cooling appreciably. However, the gases in air do not absorb IR in the range 8 to 13 microns wavelength. Any IR in this range aimed at the sky can pass through the atmosphere and leave the Earth into outer space, thereby helping to cool the Earth. Some materials have been discovered that can emit appreciable amounts of IR in the range of 8 to 13 microns wavelength such as barium sulphate ($BaSO_4$).

1. Introduction

Environmental issues such as global warming and climate change have become among the most pressing challenges faced by the current generation. These issues can be directly linked to the emission of greenhouse gases (GHG) stemming from various anthropogenic activities.[1] The sector that contributes the most by a significant amount is the energy sector, accounting for a staggering 73.2% of global GHG emissions.[2] The Intergovernmental Panel on Climate Change (IPCC) reports that at the current state of climate policies, the global mean temperature will increase by 3.2 °C by the year 2100 causing numerous adverse effects leading to widespread loss and damage to both nature and people.[3] Thus, there is an urgent need to significantly cut down on GHG emissions and explore alternatives that are able to achieve that goal.

Cooling constitutes a large percentage of the energy consumption sector in both residential and commercial applications.[4] Dong *et al.* estimated that just the cooling industry itself is responsible for over 10% of global GHG emissions and global cooling requirements are projected to at least double by 2050 due to rapid urbanization, population growth and the rise in global temperatures.[5] Passive radiative cooling is a technology whereby heat is naturally dissipated directly into deep space *via* radiation. This is achieved by emitting the heat through the sky, mainly at the wavelength interval between 8 to

[a]*Department of Chemical and Environmental Engineering, Faculty of Science and Engineering, University of Nottingham Malaysia, Jalan Broga, 43500 Semenyih, Selangor Darul Ehsan, Malaysia. E-mail: Ianatul.Khoiroh@nottingham.edu.my*
[b]*Cquestr8 Sdn. Bhd., D1105, Menara Suezcap 1, KL Gateway, Gerbang Kerinchi Lestari No 2, Jalan Kerinchi, Kuala Lumpur, Malaysia*

13 μm, which is also known as the "atmospheric window" or "sky window". At this range, almost all terrestrial thermal radiation can propagate through the atmosphere without interference, as it is highly transparent and has a significantly high atmospheric transmittance as can be seen in Fig. 1. There also exists a narrower secondary atmospheric window, between 16 to 25 μm, which could potentially be utilized for additional cooling. Its passive nature means it does not consume any electricity and has enormous potential to be utilized for the cooling of buildings, solar cells, and thermal power plants among others.[6]

Passive radiative cooling is not a new concept, in fact its applications can be traced up to several centuries back, but thorough systematic research about it had only begun in the 1960s.[7] Early research work was only limited to night-time usage, as even a small proportion of daytime solar irradiation onto a surface would negate and counteract its outgoing cooling power. The main drawback is the intrinsically low-energy density of night-time cooling which significantly limits its practical applications and would not have a meaningful impact on modern-day cooling requirements. It has been reported that under perfect conditions, night-time radiative cooling can only provide between 40–80 W m^{-2} of cooling power.[8] To achieve sufficient daytime cooling, the material must have specific properties such as an extremely low absorptivity in the highly intensive solar spectrum (0.3–2.5 μm), while at the same time possessing a high emissivity in the atmospheric window region (8–13 μm).[9] With those highly stringent requirements needed to be met, it is unsurprising why there have been little development in daytime cooling technologies only until recently.

Latest developments in radiative cooling technologies have allowed for materials or surfaces to achieve subambient temperatures even when placed under direct sunlight during the day. This is a significant achievement as it could be harnessed to minimize the use of air conditioning units for the cooling of buildings or various structures, especially in regions with a hot and sunny climate. Several methods have been proven to successfully achieve this phenomenon including manufacturing microstructure metasurfaces, selective emitters, porous structures, and random particle distribution through coatings.[10] However, most of those approaches involve complex multilayer structures that are hard to scale up and are expensive, limiting them from many applications.[11] One approach of particular interest recently is the development of radiative cooling paints because of their high reproducibility, easily scalable nature, and abundance in our modern surroundings. Researchers have developed a plethora of different radiative cooling white paints that utilize different pigments such as $BaSO_4$, $CaCO_3$, $Ca_3(PO_4)$, and MgO instead of TiO_2, which is what is commonly used in commercial white paints.

In 2021, an "ultrawhite" paint with $BaSO_4$ as its pigment was developed which has garnered global attention. It was proven to have a solar reflectance of 98.1% and was able to achieve temperatures of more than 4.5 °C below ambient temperature and a cooling power of 117 W m^{-2}.[11] A year prior to that, the same researchers also developed a cooling white paint using $CaCO_3$ as the primary pigment. It showed promising results with a solar reflectance of 95.5%, reaching temperatures of more than 1.7 °C below ambient temperatures with a cooling power exceeding 37 W m^{-2}.[12] Fig. 2 shows schematic diagram of how the radiative cooling paint works. For comparison, commercial white paints usually have a solar reflectance of between 80% to 90% and are unable to achieve subambient temperatures during the day under direct solar irradiation. Most experimental research have only been conducted in North America, where there are four seasons and a large variability of weather conditions. There has not been enough conclusive experimental works done to test the effects of these cooling paints at low latitude regions, particularly in Southeast Asia which has been theorized that passive radiative cooling can have a positive impact in Southeast Asia's tropical climate.[13] Altamimi *et al.*, explored daytime and nigh-time cooling with single layer films consisting of TiO_2, $BaSO_4$, and $BaSO_4/TiO_2$ microparticles embedded in PTFE/PVDF polymers.[14] The $BaSO_4/TiO_2$ film, exposed to direct sunlight, effectively reduced surface temperatures by approximately 4–6 °C compared to ambient conditions. Furthermore, on

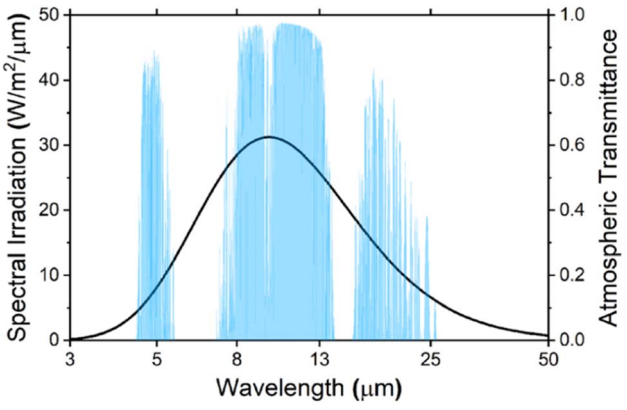

Fig. 1 Spectral irradiation of a blackbody surface at a temperature of 300 K and the atmospheric transmittance in the mid- and far-infrared regions.[6]

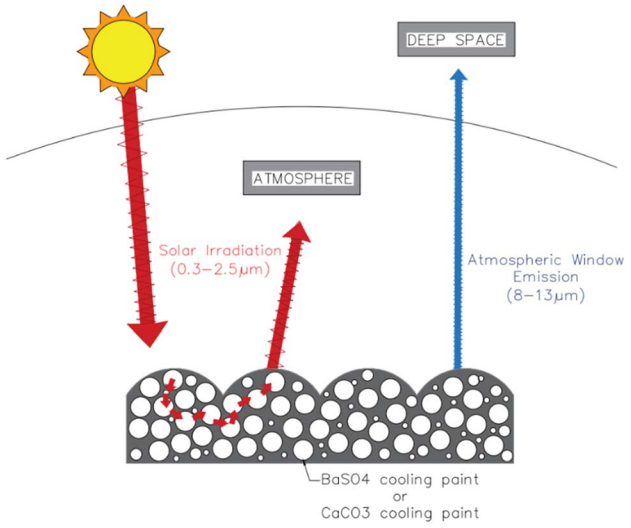

Fig. 2 Schematic diagram displaying the mechanism of radiative cooling paints.

a warm summer day, the $BaSO_4/TiO_2$/PVDF/PTFE film demonstrated an average radiative cooling power of approximately 50 W m^{-2} at 33% humidity and 46.5 W m^{-2} at 38% humidity. Atiganyanun *et al.*, tested $CaCO_3$-hollow SiO_2 with PVC binder paint for passive radiative cooling in Thailand.[15] The formulated paint performed well from 0900 to 1200, however, the ambient temperature was lower than the recorded temperatures from 1200 until 1700. The authors concluded that further investigation is required for effective passive radiative cooling.

In this work, we have conducted experimental tests to observe and quantify the effects of $BaSO_4$ and $CaCO_3$ cooling white paints under Malaysia's tropical climate. The climate in Malaysia can be characterized to be hot and humid with heavy tropical rains at certain points throughout the year. The mean annual temperature is 25.4 °C and there is relatively little seasonal variability in the temperature all year round. The mean humidity levels also range between 42% to 94%, varying from different places and months.[16] The first section of the research paper focuses on obtaining the most effective paint configuration, testing between different paint binders, solvents, and pigment concentrations. Next, a 24 hours field test was conducted to observe trends of the temperature profile of the cooling white paints against commercial white paint and the ambient temperature. The net cooling power of the cooling paints was also evaluated and the effects of various factors such as humidity levels and wind speed on the cooling performance was studied. The overall aim of this research paper is to evaluate the cooling paints performance under real-world conditions in Malaysia and determine its feasibility of widespread adoption to reduce cooling requirements within the country.

2. Methods and materials

2.1. Materials and FE-SEM analysis

The pigments used for the cooling paints include barium sulfate, $BaSO_4$ (ChemPur) and calcium carbonate, $CaCO_3$ (Sirih Pinang). Both chemicals have a purity of 100% respectively. The binders used include acrylic resin (FCPG) and epoxy resin (EveryOneShop) while the solvents used were *N*,*N*-dimethylformamide (R&M Chemicals) and distilled water. Field emission scanning electron microscopy (FE-SEM) analysis was conducted on the $BaSO_4$ and $CaCO_3$ powders to characterize their particle size distribution. The $BaSO_4$ powders had a particle size distribution of 404 ± 500 nm while the purchased $CaCO_3$ powders had a particle size distribution of 2.3 ± 2 μm. Fig. 3 shows the respective SEM images of the $BaSO_4$ and $CaCO_3$ particles. Both powders have a relatively wide particle size distribution range, which has been proven to be beneficial to efficiently scatter the wavelengths within the solar spectrum while also significantly enhancing the overall solar reflectance as opposed to a uniform particle size distribution.[11]

2.2. Fabrication of cooling paints

To fabricate the $BaSO_4$ cooling paint, the chosen solvent (dimethylformamide or water) was mixed with the $BaSO_4$ particles in a beaker placed on a stirring hot plate. The mixture was stirred constantly and heated up to approximately 70 °C. Then, the chosen resin (acrylic or epoxy) was slowly added into the mixture. Next, the mixture was ultrasonicated for 15 minutes using a UP400S Hielscher Ultrasonic Probe Mixer. This was done to reduce particle agglomerations and to introduce air bubbles into the mixture. After ultrasonication, the mixture was left to stir and be heated under the same settings as previously for another 1 hour. The constant stirring at a higher temperature was to ensure that all the chemicals were mixed thoroughly. Finally, the mixture was left to dry overnight to remove any excess solvent within the paint. To fabricate the $CaCO_3$ cooling paint, the same exact steps were conducted but substituting calcium carbonate for barium sulfate particles.

2.3. Painting methods

In the initial experiments conducted to obtain the most effective paint configuration, all the fabricated paints were painted using a paint brush. Before painting, the paints were mixed for approximately 15 minutes to ensure a uniform texture. Then, a paint brush was used to apply the first coat on the cardboard,

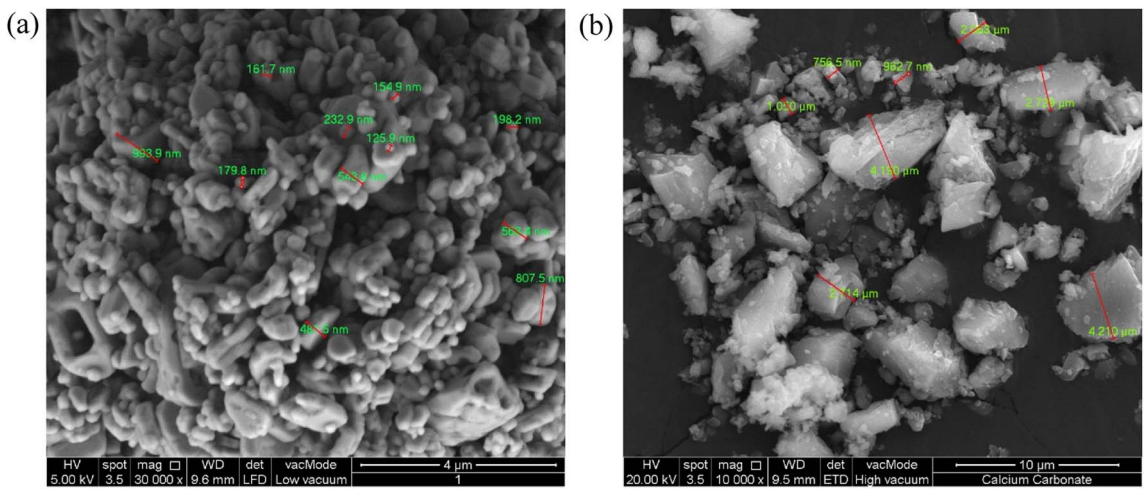

Fig. 3 SEM images of (a) $BaSO_4$ powder used in $BaSO_4$ cooling paint. (b) $CaCO_3$ powder using in $CaCO_3$ cooling paint.

it was left to dry under the sun for 30 minutes and then painted with the second coat. Once the optimum paint configuration was determined for both the $BaSO_4$ and $CaCO_3$ cooling paints, a spray gun was used to spray paint the two paints on different surfaces for the field test. To prepare the paints before spraying, they were heated up and stirred thoroughly. Additional amounts of the chosen solvent were also added to dilute the paints, to make it less viscous and more sprayable. A Ford viscosity cup was used to determine the suitable paint viscosity before spraying. Each paint type was sprayed on for a total of 5 layers of coatings. This was done to ensure that the surface was completely covered with the paint coating and to achieve more efficient radiative cooling effects. The surfaces used for the field test include wood, porcelain tiles and zinc roofing sheets.

2.4. Preliminary test setup

To determine the most optimum binder, solvent and concentration of the cooling paints, the fabricated paints were painted on a cardboard surface of approximately 20 cm × 20 cm and left to dry for a week. A sample with the chosen commercial white paint (Dulux Aura High Gloss) was also prepared and another sample which was not painted was also placed to act as a control. Then, the samples were placed under direct sunlight as can be seen in Fig. 4, and the temperatures of each sample was measured using two identical infrared thermometers (Pro'sKit MT-4606). Each test run was conducted for 1 hour, whereby the temperature measurements were manually recorded at an interval of 10 minutes. To minimize the uncertainty, each test run was repeated for 3 times on different days to ensure more reliable results. The ambient temperature was recorded using a mercury thermometer which was placed nearby the samples.

2.5. Field test setup

Four different field test setups were made to compare their different cooling performances throughout the day. A miniature house, consisting of four wooden planks as the walls, a porcelain tile as the base and a corrugated zinc sheet as the roof was created in each setup. The indoor house set up was a cube with length, width, and height of 20 cm and a roof with surface area of 31 cm × 31 cm (Fig. 5). The material for the roof was zinc, while the material for the walls was wood, and the floor inside the building was porcelain tiles. The inside temperature was measure using a laboratory digital thermometer with the sensor only in contact with the air, not any surfaces. One of the setups was left blank with no paint, another setup was painted with commercial white paint (Dulux Aura High Gloss), while the other two were painted with the $BaSO_4$ cooling paint and $CaCO_3$ cooling paint, respectively. Only the exteriors of the wooden planks were painted, as well as the top of both the porcelain tiles and zinc roofing. The field test was done to simulate real-world conditions of a building and to determine the efficiency even with the effects of surrounding factors such as convection from external wind speeds and conduction.

The setups were left out in an unshaded area for a duration of 24 hours. The temperature measurements were recorded manually at an interval of 20 minutes. A temperature sensor was placed in each of the four houses, to record the inner surrounding temperature. Meanwhile, two identical infrared thermometers (Pro'sKit MT-4606) were used to simultaneously measure the temperatures of different surfaces around the house. One infrared thermometer was used to constantly measure the temperature of the house with the commercial white paint to act as the control, while the other was used to measure the other houses separately. To measure the ambient temperature, a mercury thermometer was placed beside the houses and exposed to the surrounding environment. Fig. 6 shows the field test setups from two different angles. Local wind speed, humidity levels, and solar irradiation data were obtained from an online meteorological database (SOLCAST).[17]

2.6. Basic principles of radiative cooling

To quantify the effectiveness of a radiative cooling material, the net cooling power must be obtained. It is defined as follows:

$$P_{net} = P_{net}^{rad} - P_{non\text{-}radiative}, \quad (1)$$

where P_{net} is the net cooling power, P_{net}^{rad} is the net radiative cooling power, and $P_{non\text{-}radiative}$ denotes the nonradiative heat transfer. The equation considers the effects of both the net radiative heat transfer and the nonradiative heat transfer processes from the surrounding, such as convection and cooling. The net radiative cooling power can be further expressed as follows:

$$P_{net}^{rad} = P_{rad} - P_{atm} - P_{solar}, \quad (2)$$

Fig. 4 Preliminary test setup for the paint samples.

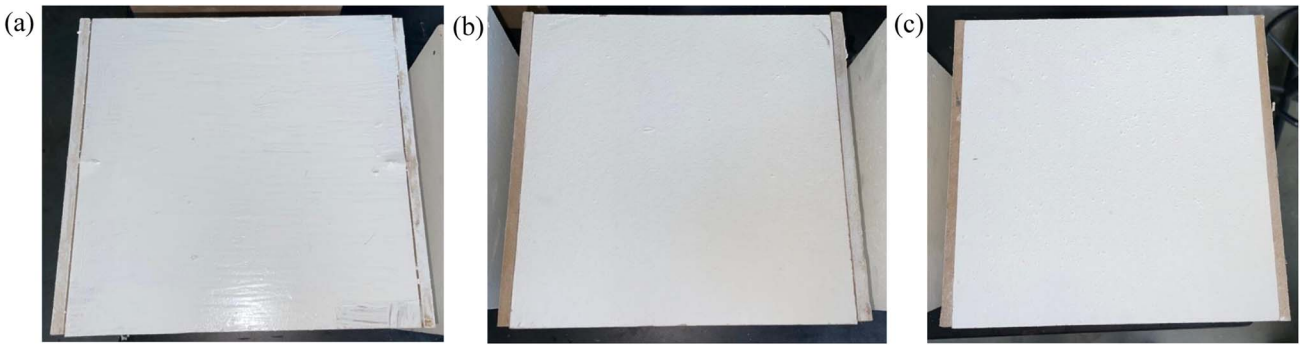

Fig. 5 Photographs of the painted wooden planks with (a) commercial white paint, (b) $CaCO_3$ cooling paint, (c) $BaSO_4$ cooling paint.

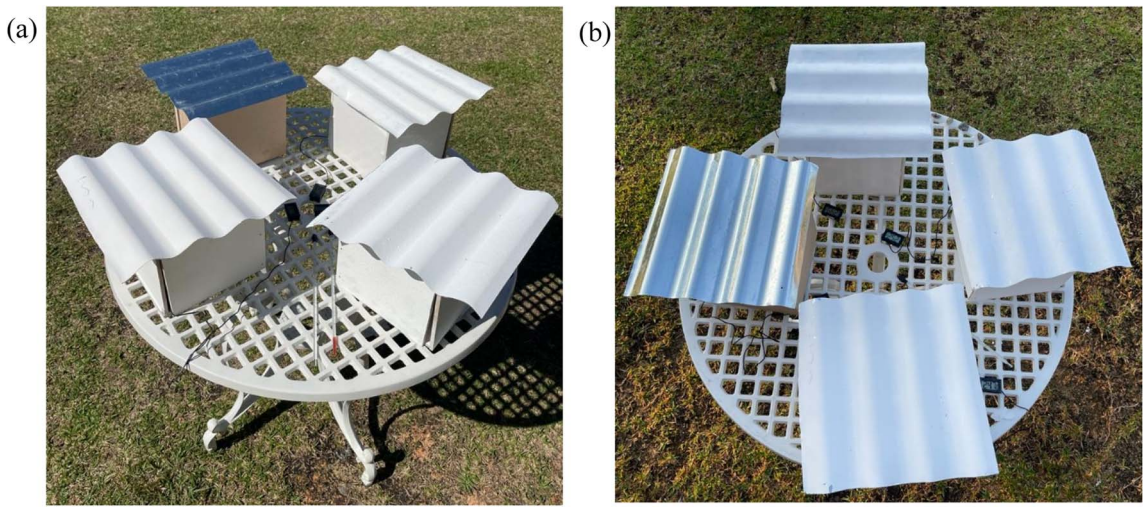

Fig. 6 Field test setups from (a) an isometric view. (b) The top view.

where P_{rad} is the thermal radiation power from the cooling surface, P_{atm} is the absorbed atmospheric radiation power on the cooling surface, and P_{solar} is the absorbed solar irradiation power on the cooling surface. Fig. 7 gives a brief overview regarding the fundamentals of radiative sky cooling. However, it was not practical to obtain the values of thermal radiation absorbed and emitted from a specific surface. Hence, to simplify the quantification of the net radiative cooling power, correlations between the net radiative cooling power and surface temperature, T_s, have been developed for both daytime and night-time respectively. They have been proven by Zhao *et al.* to be highly agreeable with actual measurement results. The correlations are as follows:

$$P_{net}^{rad} = (0.0079 \times T_s^2) + (1.27 \times T_s) + 31.6 \text{ for daytime}, \quad (3)$$

$$P_{net}^{rad} = (0.0079 \times T_s^2) + (1.27 \times T_s) + 69.9 \text{ for night-time}, \quad (4)$$

where eqn (3) and (4) are valid for surface temperatures between −10 °C and 40 °C. Meanwhile, the nonradiative heat transfer can also be further expressed as follows:

$$P_{non\text{-}radiative} = hA(T_{amb} - T_s), \quad (5)$$

where h is the overall heat transfer coefficient that accounts for both convection and conduction, A is the exposed surface area of the cooling surface, T_{amb} is the ambient temperature, and T_s is the surface temperature of the cooling surface. Since h cannot be measured directly, Zhao *et al.* also developed the following equation to quantify the nonradiative thermal loss due to wind:

$$h = (8.3 + 2.5V_{wind}), \quad (6)$$

where V_{wind} is the zero-incidence wind velocity. This equation is valid for wind speeds between 0 m s^{-1} and 8 m s^{-1}.[6]

It can be seen from the equations that in order to calculate the net cooling power of a surface, several important measurements are needed which include T_s, T_{amb}, A, and V_{wind}. Hence, all these measurements were recorded during the field tests.

The figure of merit RC was also calculated for both cooling paints. It is used to fairly evaluate the cooling radiative performance of the paints, independent of the weather conditions. It is defined as:

$$RC = \varepsilon_{sky} - r(1 - R_{solar}), \quad (7)$$

where ε_{sky} is the sky window emissivity, R_{solar} is the solar reflectance, and r is the ratio of solar irradiation over the blackbody emission through the sky window.

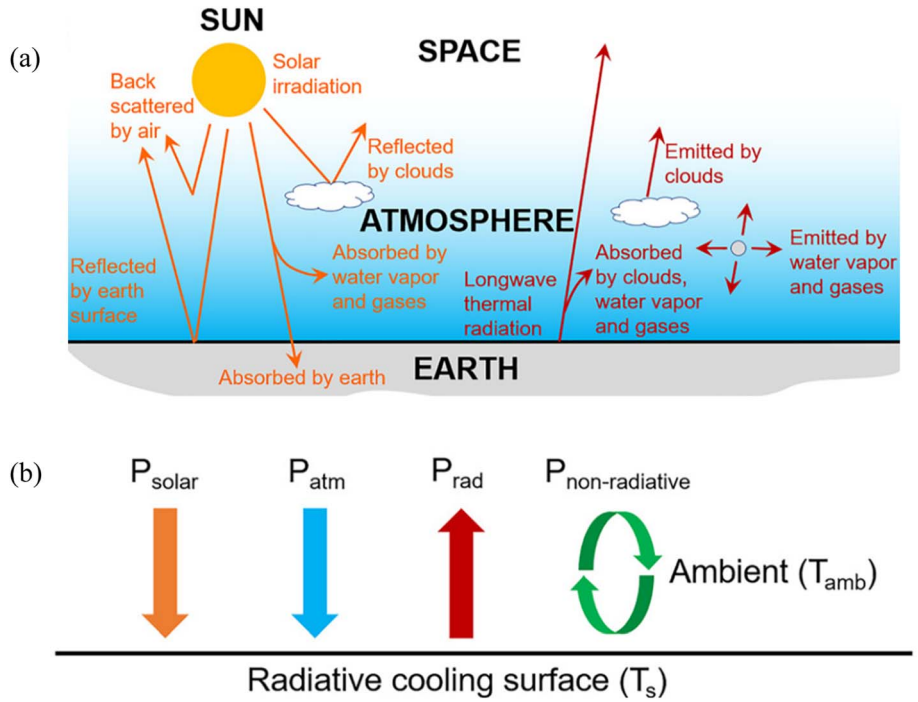

Fig. 7 Fundamentals of radiative sky cooling (a) thermal energy exchange between the Sun, Earth, space, and the atmosphere. (b) Heat transfer processes on a radiative cooling surface (Zhao *et al.*, 2019).

For the experimental results obtained, the standard deviation, σ was calculated to evaluate the variability within the measurements to determine its degree of reliability. The formula is as follows:

$$\sigma = \sqrt{\frac{\sum (X-\mu)^2}{N}} \quad (8)$$

where X denotes the value in the data distribution, μ is the population mean and N is the total number of readings.

3. Results and discussion

3.1. Determining optimum binder (acrylic *vs.* epoxy)

The first step in determining the optimum configuration of the cooling paint was to select a suitable binder. In this case, acrylic and epoxy resins were chosen as two possible candidates as they are among the most common types of binders used in commercial paints.[18] Recent developments in radiative cooling paints have proven that acrylic resin work well as binders that aids in the overall cooling performance but not many studies have been done testing epoxy resin as the binder. When bonded with the pigment, the binder should contribute to the high emissivity in the atmospheric window.[11] Fig. 8 shows the temperature comparison between $BaSO_4$-epoxy paint *vs.* $BaSO_4$-acrylic paint when placed under direct solar irradiation. Fig. 9 shows the temperature comparison between $CaCO_3$-epoxy paint *versus* $CaCO_3$-acrylic paint when placed under direct solar irradiation.

It is evident that for both pigments and both solvents, the acrylic resin has a significantly higher cooling capability than the epoxy resin. The acrylic-based paints can consistently achieve subambient surface temperatures even when placed directly

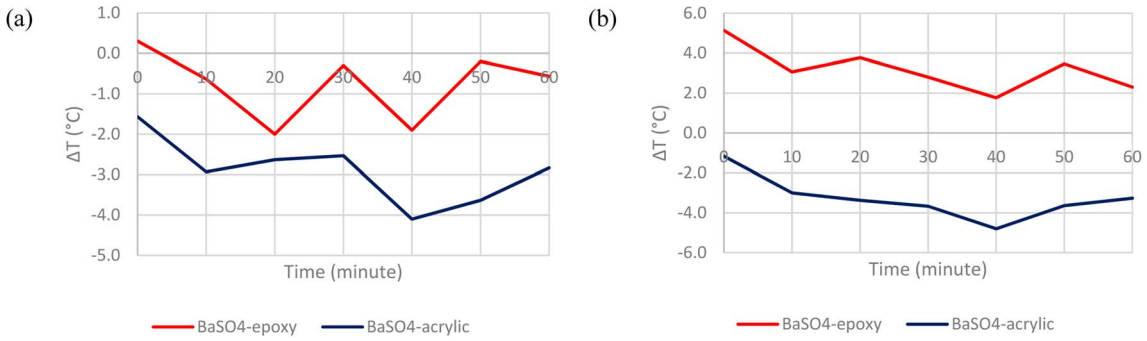

Fig. 8 Surface temperature difference with ambient temperature of (a) $BaSO_4$-epoxy paint and $BaSO_4$-acrylic paint with DMF as the solvent. (b) $BaSO_4$-epoxy paint and $BaSO_4$-acrylic paint with water as the solvent.

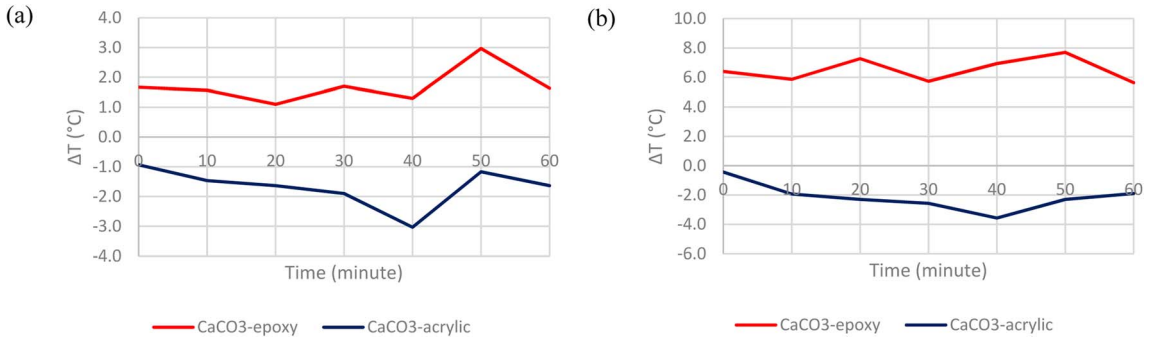

Fig. 9 Surface temperature difference with ambient temperature of (a) $CaCO_3$-epoxy paint and $CaCO_3$-acrylic paint with DMF as the solvent. (b) $CaCO_3$-epoxy paint and $CaCO_3$-acrylic paint with water as the solvent.

under the Sun. The range of subambient cooling is between −0.3 °C to −4.8 °C. In comparison, the epoxy-based paints generally absorb the solar irradiation without emitting most of it back into the atmosphere, resulting in mostly above-ambient surface temperatures. This can be attributed to the fact that the acrylic matrix introduces vibrational resonance peaks in the IR region, which ensures a higher atmospheric window emissivity while the epoxy matrix does not.[10] Hence, acrylic resin was deemed to be the more suitable binder and is chosen for the subsequent tests.

3.2. Determining optimum solvent (DMF *vs.* water)

The next step required was choosing the most suitable solvent for the cooling paints. In this experimental work, two different solvents were compared, namely dimethylformamide (DMF) and water. Previous research works into cooling paints have mostly used DMF as their preferred solvent, but water has also been suggested to be a potential alternative.[12] The two solvents may also vary depending on the application. Organic solvents such as DMF are more suited to be used as the solvent for exterior paints due to their higher resistance to extreme weather conditions and strong odour. Meanwhile, water is more suitable as the solvent for interior paints as they have low levels of volatile organic compounds (VOCs) and have little to no smell.[19] Fig. 10 shows the temperature comparison between the paints created with DMF and water as the solvent when placed under direct solar irradiation.

From the results obtained, it can be concluded that there is no clear difference between the cooling properties of the paints with different solvents. The average degree of subambient cooling for both $BaSO_4$ paints is 3 °C while both $CaCO_3$ paints is 1.7 °C. This is as expected as the solvent does not contribute in any way to the overall absorptivity or emissivity of the paint. Most, if not all of the solvent is usually evaporated once painted on the surface. Although there is no effect of the solvent on the cooling properties, DMF was still chosen as the preferred solvent due to its suitability to be painted on exterior surfaces as radiative cooling paint technologies work best under direct solar irradiation.

3.3. Determining optimum pigment concentration (50% *vs.* 60% *vs.* 70%)

The final step in finding the optimum cooling paint composition was to determine the most effective pigment concentration. The basis was set at 60% volume concentration, following what was reported by Li *et al.* with their $BaSO_4$ and $CaCO_3$ cooling paints. It is a much higher concentration than what is commonly used in commercial paints. This was done because a high pigment concentration is needed to overcome the low refractive index of the pigments themselves.[11] A variation of ±10% relative to the basis concentration was adopted, resulting in a comparison between pigment volume concentrations of 50%, 60% and 70%. Fig. 11 shows the temperature comparison for both $BaSO_4$ and $CaCO_3$ cooling paints at different concentrations.

For $BaSO_4$ cooling paints, the results indicated that there was not a significant difference between the degree of subambient

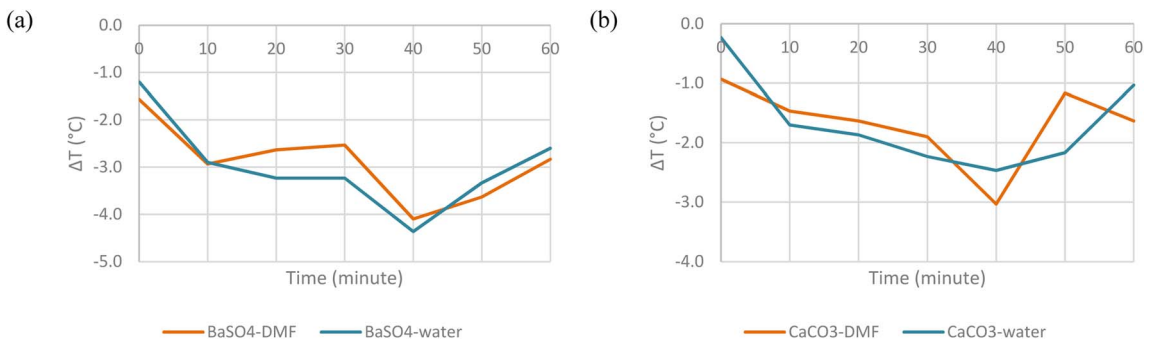

Fig. 10 Surface temperature difference with ambient temperature of (a) $BaSO_4$-DMF paint and $BaSO_4$-water paint. (b) $CaCO_3$-DMF paint and $CaCO_3$-water paint.

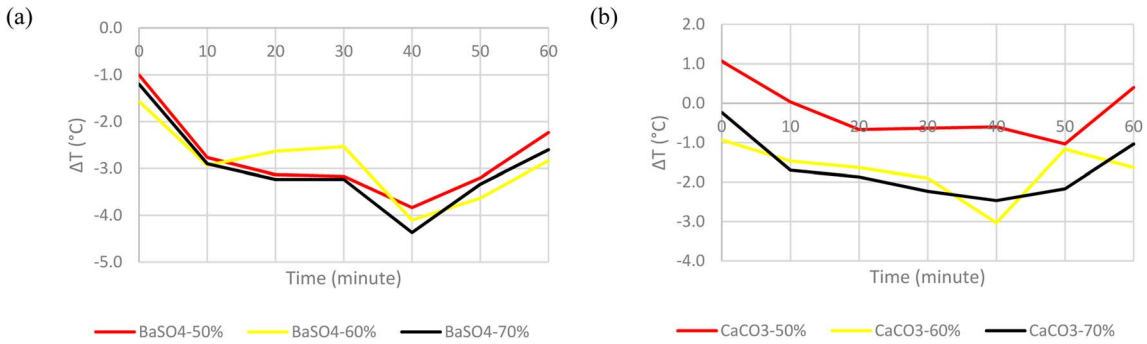

Fig. 11 Surface temperature difference with ambient temperature of (a) $BaSO_4$ cooling paint at three different concentrations. (b) $CaCO_3$ cooling paint at three different concentrations.

Table 1 Comparison of $BaSO_4$ cooling paints at different concentrations

Volume concentration (%)	Mean temperature difference (°C)	Standard deviation
50	−2.8	1.105
60	−2.9	1.112
70	−3.0	1.546

Table 2 Comparison of $CaCO_3$ cooling paints at different concentrations

Volume concentration (%)	Mean temperature difference (°C)	Standard deviation
50	−0.2	1.648
60	−1.7	1.516
70	−1.7	1.190

cooling for the different concentrations. The mean temperature difference was only within ±0.2 °C for all three samples. Hence, to determine the most optimum concentration, the standard deviation of all the measurements was also considered. Eqn (8) was used to calculate the standard deviation values. The volume concentration of 60% was chosen as it had a good degree of subambient temperature reduction as well as a relatively low standard deviation. A summary of the results obtained from the three $BaSO_4$ samples can be seen in Table 1.

The $CaCO_3$ cooling paints on the other hand, showed a slightly different trend. The lower concentration of 50% showed a significantly lower degree of subambient cooling, with some of the measurements even being at above ambient temperatures. A possible explanation for this is because at 50% $CaCO_3$ volume concentration, the texture of the paint sample fabricated was too runny and not suitable to be brushed on the cardboard surface, the trends for both 60% and 70% volume concentration are more comparable with one another with both samples recording the same mean temperature difference. Nevertheless, the volume concentration of 70% was deemed more suitable as it had a lower standard deviation. Table 2 shows a summary of the results obtained from the three $CaCO_3$ samples.

From the previous tests, the optimum composition and configuration of the cooling paints was determined. They were then fabricated and used to proceed with the field test. A summary of the two different paint types can be seen in Table 3.

3.4. Performance of cooling paints on different surfaces

The cooling paints were tested against commercial white paint (Dulux Aura High Gloss) on several different types of surfaces including cardboard, wood, zinc, tin, and porcelain. Different surfaces were tested to determine which material would be the most suitable for cooling paints to be applied upon. The tests

Table 4 Summary of cooling paint performance on different surface types

	Mean temperature difference (°C)		Minimum temperature reduction (°C)		Maximum temperature reduction (°C)	
Surface type	$BaSO_4$	$CaCO_3$	$BaSO_4$	$CaCO_3$	$BaSO_4$	$CaCO_3$
Cardboard	−2.9	−2.1	−0.7	−0.3	−6.2	−5.9
Wood	−3.9	−3.0	−1.3	−0.8	−5.9	−5.6
Zinc	−3.2	−4.0	−0.2	−0.5	−6.3	−9.2
Tin	−4.7	−2.9	−1.1	−0.2	−9.8	−5.5
Porcelain	−3.6	−2.8	−0.8	−1.3	−6.4	−3.9

Table 3 Summary of optimum cooling paint configurations

Name	Pigment	Particle size (nm)	Binder	Solvent	Volume concentration (%)
$BaSO_4$ cooling white paint	$BaSO_4$	404 ± 500	Acrylic resin	DMF	60
$CaCO_3$ cooling white paint	$CaCO_3$	2300 ± 2000	Acrylic resin	DMF	70

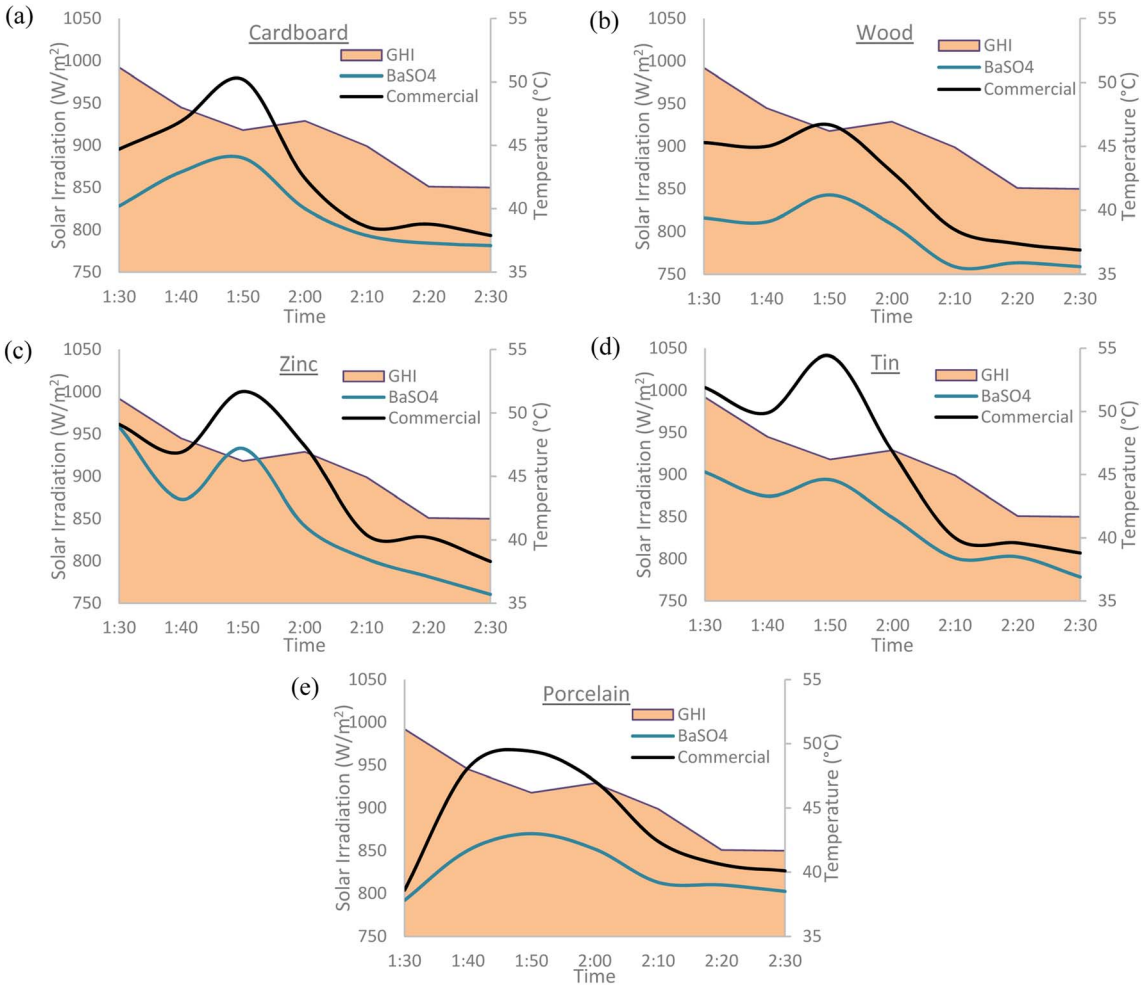

Fig. 12 Surface temperature comparison of $BaSO_4$ cooling paint and commercial white paint for (a) cardboard, (b) wood, (c) zinc, (d) tin, (e) porcelain. All measurements were taken on 8th March 2023 in Semenyih, Malaysia.

were conducted at times with peak solar irradiation during the day with all the surfaces being placed directly under the Sun. The results obtained showed that both cooling paints considerably outperformed the commercial white paint on every surface type with the $BaSO_4$ cooling paint yielding the best results. The results are summarized in Table 4 and the trends can clearly be seen in Fig. 12 and 13. GHI denotes the global horizontal irradiance which is the value of total solar radiation incident on a horizontal surface. The GHI data was obtained from SOLCAST, an online meteorological database.

It is evident that the cooling paints have a better performance on certain surface types more than others. However, it was not possible to conclude a definitive relationship between the surface type and the cooling paint performance. Further experimental work and investigation is required.

3.5. Field test results (comparison with ambient temperature)

The field test results, as shown in Fig. 14, show that both the $BaSO_4$ and $CaCO_3$ cooling paints displayed remarkable 24 hours long subambient temperatures, even when placed directly under the Sun during the day. In fact, the biggest subambient temperature difference occurs when the solar irradiation is at its highest. The range of subambient temperature difference for the $BaSO_4$ cooling paint was between −0.2 °C to −6.1 °C while for the $CaCO_3$ cooling paint, the range was between −0.2 °C to −6 °C. Throughout nighttime, there was relatively little subambient temperature difference, mainly due to the lack of solar irradiation and the high relative humidity levels. The performance of both cooling paints was comparable, with the $BaSO_4$ paint having a mean daytime subambient temperature difference of −2.6 °C while the $CaCO_3$ paint was −2.5 °C.

To consistently achieve subambient surface temperatures, it is essential to have a high solar reflectance and high emissivity in the atmospheric window. The high solar reflectance is usually contributed by the pigment particles while the high emissivity can come from either the pigment particles and/or the matrix (combination of pigment and binder). The remarkable performance of both cooling paints can be attributed to the properties of the respective pigments (*i.e.*, refractive index, volume concentration, particle size and particle size distribution). For $BaSO_4$ particles, the high electron band gap of ~6 eV

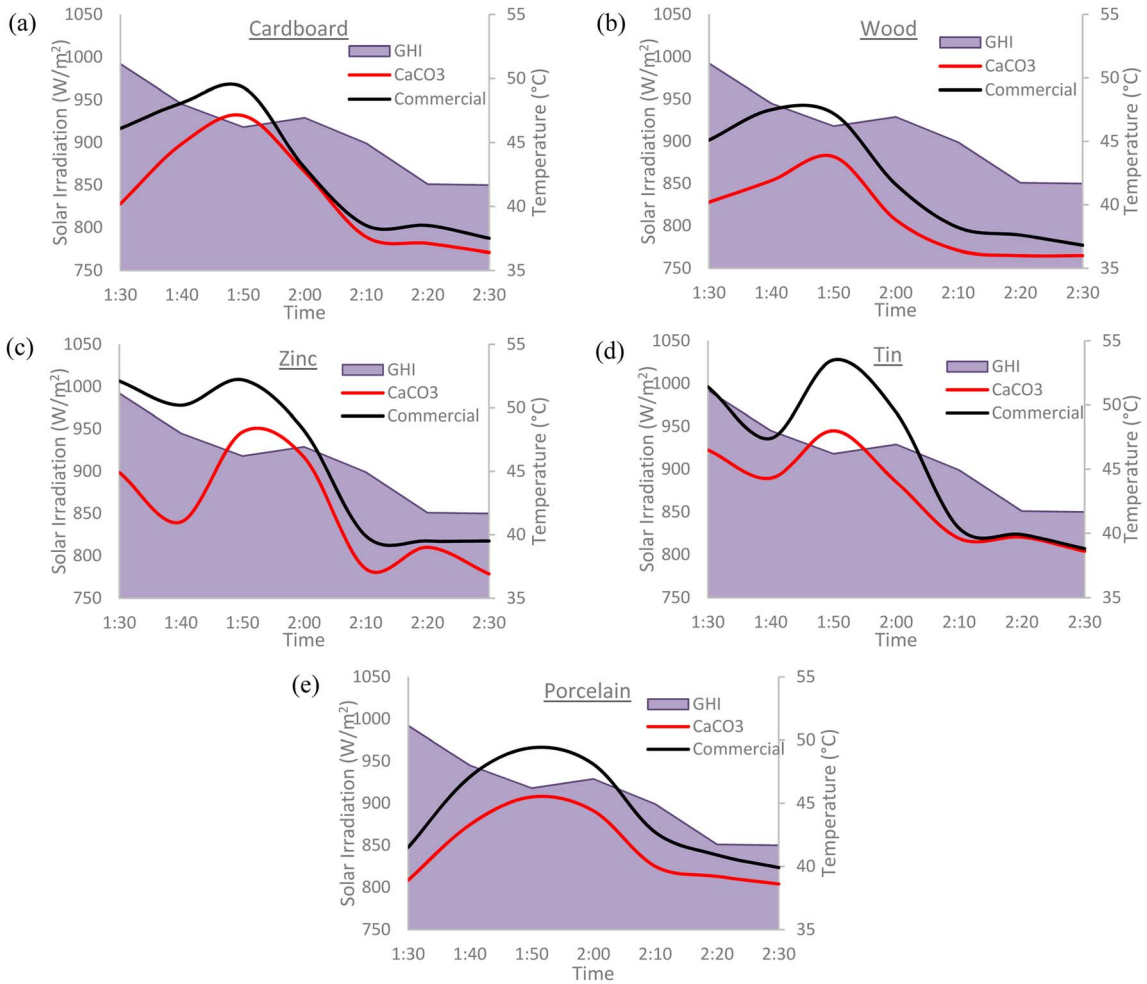

Fig. 13 Surface temperature comparison of $CaCO_3$ cooling paint and commercial white paint for (a) cardboard, (b) wood, (c) zinc, (d) tin, (e) porcelain. All measurements were taken on 8th March 2023 in Semenyih, Malaysia.

contributes to the reduced absorption in the Ultraviolet (UV) band while phonon resonance of the particles also occurs at 9 μm, which is within the atmospheric window.[11] As for the $CaCO_3$ particles, the electron band gap is also relatively high at around >5 eV which also reduces the UV absorption.[12]

A key challenge faced when utilizing both pigments in paints is their low refractive index which causes a decrease in the scattering effect when compared to commercial pigments such as TiO_2.[20] To overcome this, a relatively higher pigment volume concentration had to be adopted, namely 60% for $BaSO_4$ and 70% for $CaCO_3$. In comparison, commercial white paints usually have pigment volume concentrations ranging from 5–25%, depending on the specific type.[21] A higher pigment volume concentration in turn also reduces the volume concentration of the binder. Which aids in reducing the overall absorption in the NIR region. Another method employed to overcome the low refractive index was to adopt a large particle size distribution. Based on the FE-SEM analysis, both pigments had a distribution of approximately ±100% of the mean particle size. This aids in increasing the efficiency of scattering the wavelengths in the solar spectrum. As mentioned previously, the presence of the acrylic matrix ensures that the cooling paints have a higher atmospheric window emissivity as it introduces resonance peaks in the IR region.[10]

3.6. Field test results (comparison with commercial paint)

When compared to commercial white paint (Dulux Aura High Gloss), both $BaSO_4$ and $CaCO_3$ cooling paints demonstrated significant cooling performance during the daytime when solar irradiation is present. The temperature difference with commercial paint reached up to −9.6 °C for $BaSO_4$ cooling paint and up to −6.5 °C for $CaCO_3$ cooling paint when a peak solar irradiation value of 922 W m^{-2} was observed. The mean daytime difference with commercial throughout the day was −2.9 °C for $BaSO_4$ cooling paint and −2.7 °C for $CaCO_3$ cooling paint. The temperature profiles were more comparable during night-time with little to no difference between the surface temperatures as can be seen in Fig. 15.

The significant increase in commercial paint surface temperatures under solar irradiation can be attributed to the pigment (TiO_2) having a moderate 3.2 eV electron band gap which increases the overall solar absorption in the UV band. The higher volume concentration of the acrylic binder also increases the solar absorption in the NIR region, thus further

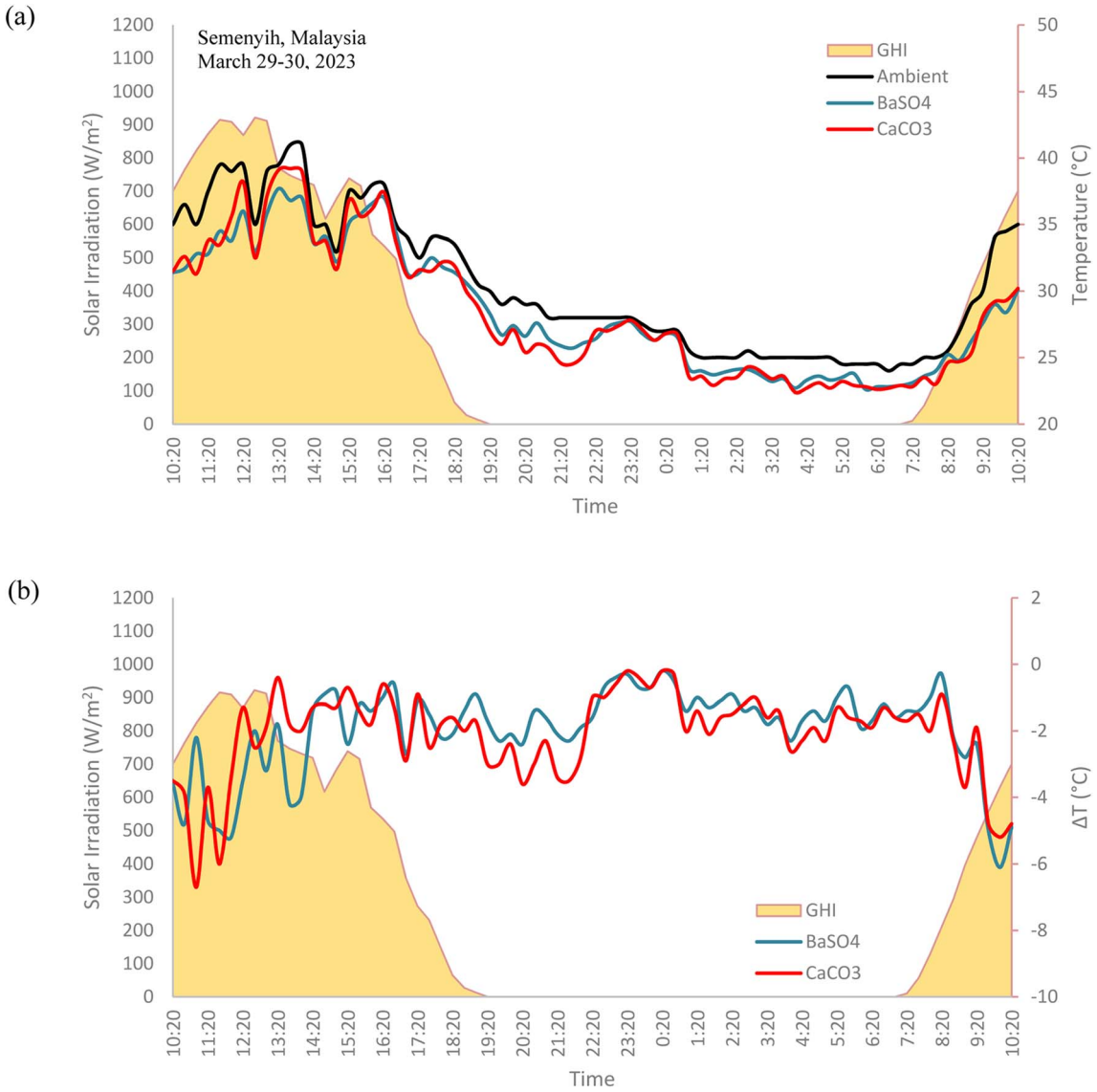

Fig. 14 Field test results of (a) $BaSO_4$ cooling paint, $CaCO_3$ cooling paint and ambient temperatures. (b) Temperature difference with ambient for $BaSO_4$ cooling paint and $CaCO_3$ cooling paint.

increasing the surface temperature. These factors lead to the reduction of the paint's solar reflectance, hindering its cooling properties. Based on theoretical studies and simulation, it was estimated that TiO_2-based paints are unlikely to exceed a solar reflectance value of 92%, hence would not be a good candidate in achieving daytime subambient temperatures.[12]

3.7. Net radiative cooling power of $BaSO_4$ and $CaCO_3$ cooling paints

The net radiative cooling power of both cooling paints were calculated using eqn (1), taking into consideration the effects of both the radiative and non-radiative heat transfer processes. The average cooling power of the $BaSO_4$ cooling paint was 71.0 W m^{-2} while the $CaCO_3$ cooling paint was 69.9 W m^{-2}. The average daytime cooling power of both paints were 47.5 W m^{-2} and 48.8 W m^{-2} respectively. As can be seen in Fig. 16, the net cooling power is typically higher during the night-time as there is no solar irradiation present which usually counteracts some of the radiative cooling performance during the day. A variety of factors can affect the net cooling power of the cooling paints including the humidity levels, wind speed, cloud opacity and the zenith angle.[22]

It is important to note that the net cooling power here is lower than those reported in recent research works regarding radiative cooling paints which are typically in the range of above 100 W m^{-2}.[10,11] There is a plethora of reasons why including the different climate conditions, ambient temperature, solar irradiation, *etc.* but by far the most significant factor is the non-radiative heat transfer effects. The experimental setup done in this work does not utilize any convection shield to cover the radiative cooling surface, like what is usually done in other research works. It was purposely done to see how radiative cooling paints would perform under real-life conditions, whereby any form of convection shield would not usually be

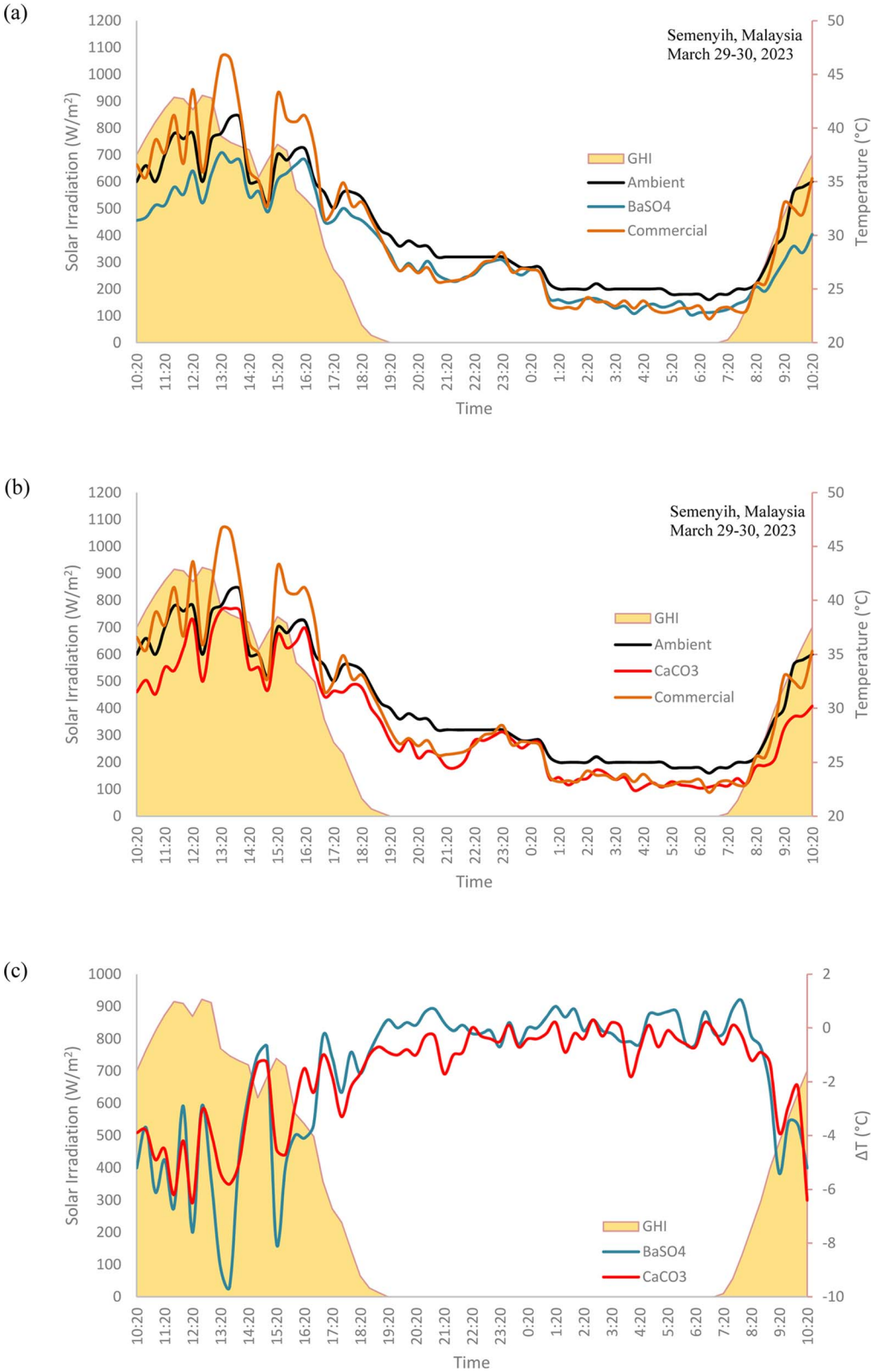

Fig. 15 Field test results of (a) $BaSO_4$ cooling paint, commercial paint, and ambient temperatures. (b) $CaCO_3$ cooling paint, commercial paint, and ambient temperatures. (c) Temperature difference with commercial for $BaSO_4$ cooling paint and $CaCO_3$ cooling paint.

present. This can cause a considerable portion of the cooling power to be lost through convection and conduction. Fig. 17 shows the net cooling power performance of the individual cooling paints and their temperature profile. Further research works are needed to develop a method to reduce the non-radiative transfer effects towards radiative cooling paints.

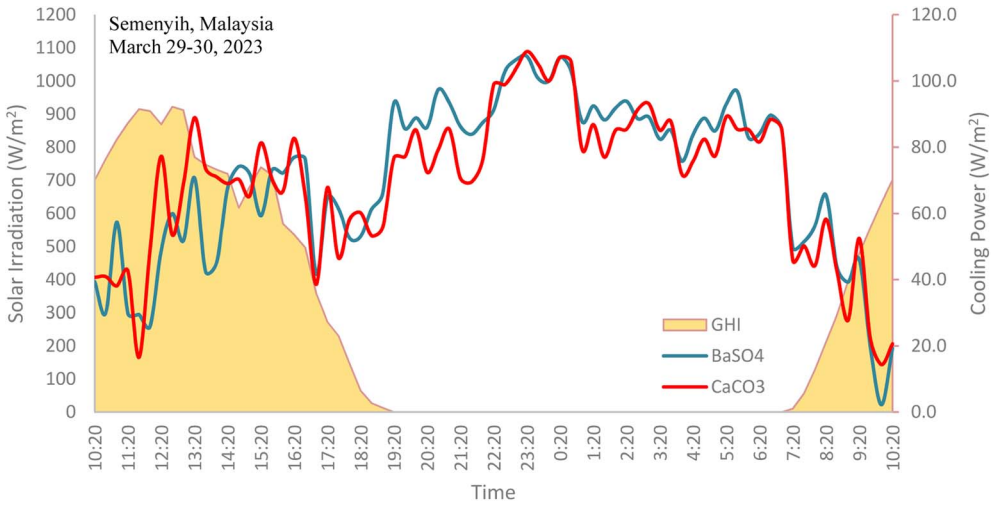

Fig. 16 Field test results showing the net cooling powers of $BaSO_4$ cooling paint and $CaCO_3$ cooling paint.

Fig. 17 Net cooling power performance and the temperature profiles of (a) $BaSO_4$ cooling paint. (b) $CaCO_3$ cooling paint.

Nevertheless, the results obtained by the cooling paints in Malaysia show great potential and can bring substantial benefits if adopted properly and at a large scale.

3.8. Effect of various climate factors on net radiative cooling power

The humidity levels also play a significant role affecting the net cooling power of the radiative cooling surface. Based on Fig. 18, when plotted against the relative humidity, there is an inverse relationship between the net cooling power and humidity. As the relative humidity increases, the water vapour content in the air also increases. This in turn reduces the amount of heat that can be radiated to the surroundings by the cooling paints as water vapour interferes by absorbing and re-emitting the long-wave radiation emitted.[23] With water vapour being the most prominent source of IR absorption in the atmosphere, the increase in water vapour causes the decrease of atmospheric transmittance and the increase of spectral irradiance in the atmospheric window. Thus, leading to the cooling paint absorbing more atmospheric radiation and limiting its cooling performance.[24] It was also suggested that in warm humid environments like in Malaysia, the high humidity and precipitable water vapor (PWV) levels causes the secondary atmospheric window (16 to 25 μm) to close.[25] This would inevitably

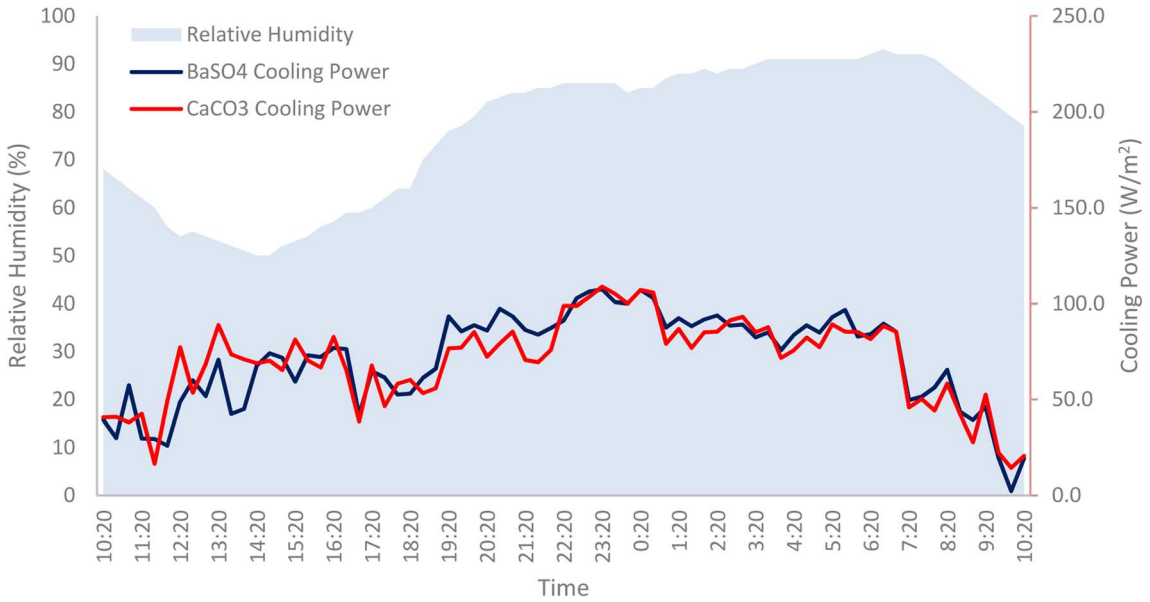

Fig. 18 Relative humidity levels plotted against the cooling powers of $BaSO_4$ cooling paint and $CaCO_3$ cooling paint.

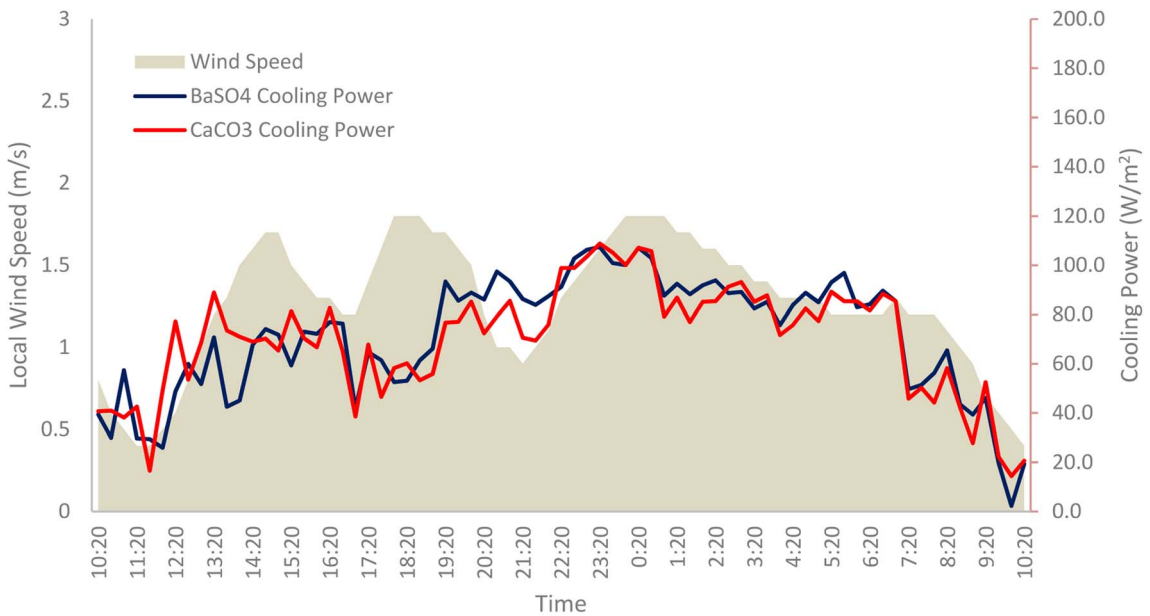

Fig. 19 Local wind speeds plotted against the cooling powers of $BaSO_4$ cooling paint and $CaCO_3$ cooling paint.

hinder any potential additional cooling power obtained from radiative cooling surfaces.

The local wind speed, V_{wind} also plays a crucial role in the non-radiative heat transfer processes, as is evident from eqn (6) with the correlation for the local heat transfer coefficient being directly proportional to V_{wind}. Heat transfer through convection may either be beneficial or detrimental to the radiative cooling device, depending on the application. For subambient applications, such as this, it can be detrimental and needs to be suppressed as much as possible.[26] A higher local wind speed will aggravate the free convection heat transfer from the cooling paint surface with the surrounding warmer air.[27] Fig. 19 shows a plot of the local wind speeds against the calculated net cooling power obtained from the field test.

On average, the non-radiative heat transfer effects account for approximately 25–26% of the loss in the net cooling power of both cooling paints. Thus, there is a dire need to minimize these losses in real world applications to achieve maximum cooling performance and efficiency. Clearly, it is not possible to alter the weather conditions at a certain location, and the most practical solution would be to install some form of convection shield to insulate the top of the surface that faces the sky and the incoming solar irradiation. Liu *et al.*, proposed employing a "tilt strategy and wind cover strategy" to minimize the effects of the non-radiative heat exchange caused by the winds.[28]

While it may not be a practical solution to apply for the painting of buildings, it could be utilized to improve the performance of a wide range of heat exchangers, including air fin coolers and external radiators of air-conditioning systems. A suitable insulating material would need to have a few key characteristics including a high transmittance across the entire infrared (IR) band, high mechanical strength to persist through harsh weather conditions, high durability as well as a relatively low cost.[29] Such a material that possesses all these characteristics is yet to be developed, but the closest solution currently is utilizing a polyethylene (PE) film.[30] Further investigation and research are needed to realize the full potential of radiative cooling paints.

Several other factors also play a key role affecting the net radiative cooling power of both the cooling paints. A high cloud coverage during the day would significantly reduce the amount of solar irradiation directed onto a cooling surface, thus hindering its overall emissivity and net cooling power.[31] Rain is another crucial factor, which can have a beneficial or detrimental impact on the cooling performance. Moderate rain could actually help clean the radiative cooling surfaces that have been covered with dust, dirt or any debris and improve its overall reflectivity. On the other hand, continuous heavy rain would result in water accumulation on the surface, which can significantly hinder its cooling performance.[32] The scope of this research work does not fully study these factors and further investigation is required.

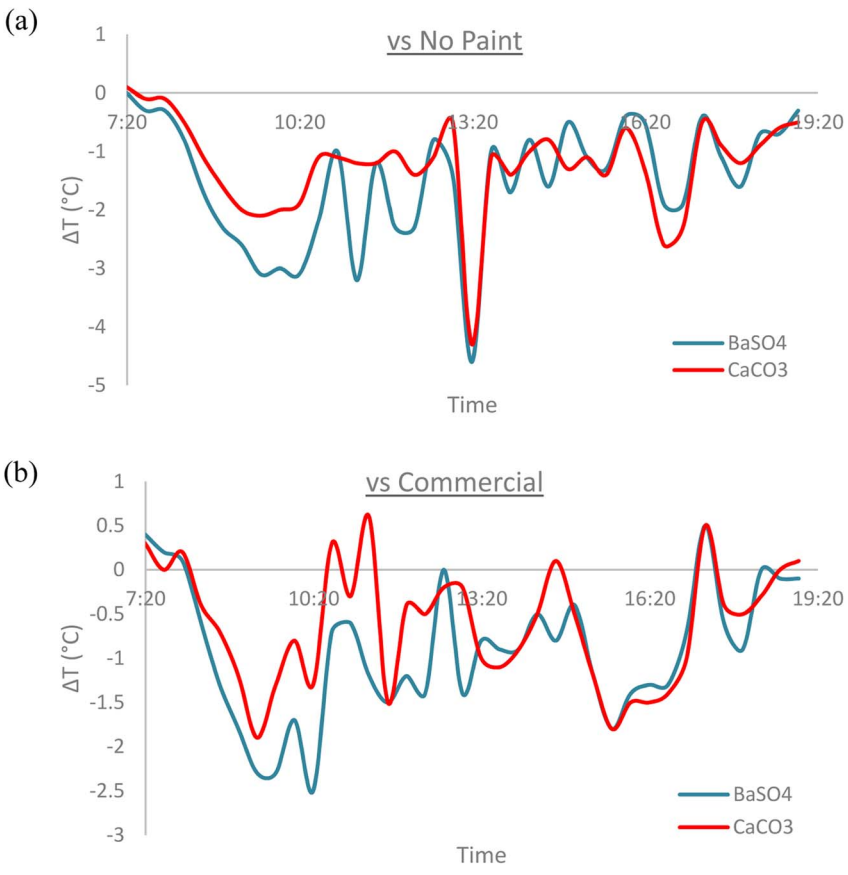

Fig. 20 Indoor temperature difference during the daytime with (a) "No Paint" house for both cooling paints. (b) "Commercial" house for both cooling paints.

Table 5 Comparison of $BaSO_4$ cooling paint and $CaCO_3$ cooling paint

Parameter	$BaSO_4$ cooling paint	$CaCO_3$ cooling paint	Difference (%)
Reported solar reflectance (%)	98.1 (ref. 11)	95.5 (ref. 12)	2.65
Reported sky window emissivity	0.95 (ref. 11)	0.94 (ref. 12)	1.05
Minimum subambient temperature reduction (°C)	−0.2	−0.2	0
Maximum subambient temperature reduction (°C)	−6.1	−6	1.64
Mean subambient temperature reduction (°C)	−2.0	−2.0	0
Mean daytime net cooling power (W m^{-2})	47.5	48.8	2.74
Mean night-time net cooling power (W m^{-2})	91.3	86.5	5.26
Mean net cooling power (W m^{-2})	71.0	69.9	1.55
RC figure of merit	0.68	0.42	38.38

3.9. Indoor house temperature results

Miniature houses were built as part of the field test setup to observe the indoor cooling effects of the cooling paints *vs.* commercial white paint (Dulux Aura High Gloss) as well as a house without any paint (No Paint). As expected, the house with no paint recorded the highest indoor temperature throughout the daytime when solar irradiation was present. The mean temperature reduction recorded during the daytime when compared to "No Paint" was −1.5 °C for $BaSO_4$ cooling paint and −1.2 °C for $CaCO_3$ cooling paint, reaching a peak temperature difference of −4.6 °C and −4.3 °C respectively. When compared against the "Commercial White Paint" house, the mean temperature reduction recorded during the daytime was −0.9 °C for $BaSO_4$ cooling paint and −0.6 °C for $CaCO_3$ cooling paint, reaching a peak temperature difference of −2.5 °C and −1.9 °C respectively. Fig. 20 shows the temperature difference between the cooling paint houses with the other house setups.

If employed on a larger scale with an even bigger cooling surface area, it is expected that the cooling performance would remain similar. While this is clearly not enough to negate the need of air conditioning, especially in a warm and humid country like Malaysia, the cooling paints are able to act as a supplement to further decrease cooling energy demands.[33] Interest in passive radiative cooling technologies, especially paint coatings, will only continue to increase in the near future due to its cost saving attributes.[34]

3.10. Performance comparison of $BaSO_4$ and $CaCO_3$ cooling paints

Based on the performance of both cooling paints, it is undeniable that the $BaSO_4$ cooling paint shows consistently better cooling performance throughout all the tests conducted, compared to the $CaCO_3$ cooling paint. Nevertheless, the differences between both the cooling paints are not too significant, as they have a very small percentage difference for a majority of the parameters. The reported higher solar reflectance and sky (atmospheric) window emissivity values of the $BaSO_4$-acrylic paint helps it edge out the $CaCO_3$-acrylic paint in terms of cooling performance. From a visual perspective, the $BaSO_4$ cooling paint also has a more distinct whiter colour, with Li *et al.* dubbing it as "ultrawhite" whereas the $CaCO_3$ cooling paint has a slight greyish tint in the overall white colour.[11] $BaSO_4$ cooling paint also outperformed the $CaCO_3$ on a majority of the different surface types including cardboard, tin, wood and porcelain. Table 5 shows a summary of the results obtained from both paints. The figure of merit RC was calculated using eqn (7). The r value was taken to be 10 as a 300 K blackbody emission was assumed.

Overall, it is safe to conclude that $BaSO_4$ cooling paint is the preferred choice rather than the $CaCO_3$ cooling paint. The only benefit that would arise from adopting $CaCO_3$ as the preferred cooling paint pigment is its lower cost when compared to pure $BaSO_4$. That may also be a key factor of consideration if widespread and large-scale implementation of radiative cooling paints were to occur. Further investigation should be conducted to find ways to improve the efficiency of cooling paints in tropical climates like in Malaysia.

4. Conclusion

To sum up, two types of cooling paints were fabricated utilizing $BaSO_4$ and $CaCO_3$ as the respective pigments. After testing, the most optimum cooling paint configuration consisted of acrylic resin acting as the binder and dimethylformamide (DMF) as the solvent. For the $BaSO_4$ cooling paint, the volume concentration of the pigment was set at 60% while the volume concentration for the $CaCO_3$ cooling paint was set at 70%, both of which are significantly higher than the pigment concentration of commercial paints. Both cooling paints possess a remarkably high solar reflectance and emissivity in the atmospheric window (8–13 μm), allowing it to retain the temperature of painted surfaces to even below ambient temperature levels. The paints were also tested against commercial white paint (Dulux Aura High Gloss) on various types of surfaces (*i.e.*, cardboard, wood, zinc, tin, and porcelain) and showed considerably lower surface temperatures for each material.

The field test results showed that both cooling paints were able to achieve remarkable subambient temperatures throughout the entire day, even when placed under direct solar irradiation during daytime. The $BaSO_4$ cooling paint achieved a mean subambient temperature reduction of −2 °C, a peak of −6.1 °C and a mean cooling power of 71.0 W m^{-2} while the $CaCO_3$ cooling paint yielded a mean temperature reduction of −2 °C, a peak of −6 °C and a mean cooling power of 69.9 W m^{-2}. When compared

against various climate factors, it was concluded that the net cooling power of the paints had an inverse relationship with both the relative humidity levels and the local wind speed. The heat transfer through non-radiative processes such as conduction and convection accounted for a considerable percentage of the net cooling power reduction. The indoor temperatures of the miniature houses were also consistently lower for both cooling paints compared to commercial white paint as well as no paint during the daytime. Between the two, the $BaSO_4$ cooling paint yielded consistently better results compared to the $CaCO_3$ cooling paint and is deemed more favourable due to its higher cooling performance as well as its whiter appearance.

There are many challenges posed by the climate conditions in Malaysia when attempting to optimize the cooling performance of both paints. The high humidity levels, local wind speed and frequent tropical rains can be detrimental to their performance. Nevertheless, this experimental work yielded very promising results. A maximum subambient temperature reduction of −6.1 °C and −6 °C under peak solar irradiation and an average daytime cooling power of 47.5 W m^{-2} and 48.8 W m^{-2} for the $BaSO_4$ cooling paint and $CaCO_3$ cooling paint respectively, is already a remarkable feat. While the radiative cooling paints would be most efficient under dry and warm weather conditions such as in desert climates, its effects in Malaysia's tropical climate may also prove to be significant in reducing the active cooling requirements and energy consumption within the region.

Conflicts of interest

There are no conflicts of interest to declare.

Acknowledgements

The authors gratefully acknowledge the financial support from the Department of Chemical and Environmental Engineering, University of Nottingham Malaysia. A. K. K. acknowledges financial support for a postdoc fellowship through the NVEC0022 grant from Cquestr8 Sdn. Bhd. The authors also thank Qisya Izanti for her help in the sample fabrication process and field test.

References

1 A. Mikhaylov, N. Moiseev, K. Aleshin and T. Burkhardt, Global Climate Change And Greenhouse Effect, *Entrep. Sustain. Issues*, 2020, **7**, 2897–2913.

2 H. Ritchie, M. Roser and P. Rosado, *CO_2 and Greenhouse Gas Emissions*, Our World in Data [Internet]. 2020 May 11 [cited 2023 Mar 31], available from: **https://ourworldindata.org/co2-and-greenhouse-gas-emissions**.

3 *Climate Change 2022: Impacts, Adaptation and Vulnerability*, [Internet]. [cited 2023 Mar 31], available from: **https://www.ipcc.ch/report/ar6/wg2/**.

4 J. Conti, P. Holtberg, J. Diefenderfer, A. LaRose, J. T. Turnure and L. Westfall, *International Energy Outlook 2016 with Projections to 2040*, 2016 May 1 [cited 2023 Mar 31], available from: **http://www.osti.gov/servlets/purl/1296780/**.

5 Y. Dong, M. Coleman and S. A. Miller, Greenhouse Gas Emissions from Air Conditioning and Refrigeration Service Expansion in Developing Countries, *Annu. Rev. Environ. Resour.*, 2021, **46**, 59–83, DOI: **10.1146/annurev-environ-012220-034103**.

6 D. Zhao, A. Aili, Y. Zhai, S. Xu, G. Tan, X. Yin, *et al.*, Radiative sky cooling: Fundamental principles, materials, and applications, *Appl. Phys. Rev.*, 2019, **6**(2), 021306.

7 M. N. Bahadori, Passive Cooling Systems in Iranian Architecture, *Sci. Am.*, 1978, **238**(2), 144–154, available from: **https://www.scientificamerican.com/article/passive-cooling-systems-in-iranian**.

8 U. Eicker and A. Dalibard, Photovoltaic–thermal collectors for night radiative cooling of buildings, *Sol. Energy*, 2011, **85**(7), 1322–1335.

9 J. Mandal, Y. Fu, A. C. Overvig, M. Jia, K. Sun, N. N. Shi, *et al.*, Hierarchically porous polymer coatings for highly efficient passive daytime radiative cooling, *Science*, 2018, **362**(6412), 315–319, DOI: **10.1126/science.aat9513**.

10 J. Lv, Z. Chen and X. Li, Calcium Phosphate Paints for Full-Daytime Subambient Radiative Cooling, *ACS Appl. Energy Mater.*, 2022, **5**(4), 4117–4124, DOI: **10.1021/acsaem.1c03457**.

11 X. Li, J. Peoples, P. Yao and X. Ruan, Ultrawhite BaSO4Paints and Films for Remarkable Daytime Subambient Radiative Cooling, *ACS Appl. Mater. Interfaces*, 2021, **13**(18), 21733–21739, DOI: **10.1021/acsami.1c02368**.

12 X. Li, J. Peoples, Z. Huang, Z. Zhao, J. Qiu and X. Ruan, Full Daytime Sub-ambient Radiative Cooling in Commercial-like Paints with High Figure of Merit, *Cell Rep. Phys. Sci.*, 2020, **1**(10), 100221.

13 K. M. Al-Obaidi, M. Ismail and A. M. Abdul Rahman, Passive cooling techniques through reflective and radiative roofs in tropical houses in Southeast Asia: a literature review, *Front. Archit. Res.*, 2014, **3**(3), 283–297.

14 M. M. S. Altamimi, U. Saeed and H. Al-Turaif, BaSO4/TiO2 Microparticle Embedded in Polyvinylidene Fluoride-Co-Hexafluoropropylene/Polytetrafluoroethylene Polymer Film for Daytime Radiative Cooling, *Polymers*, 2023, **15**, 3876.

15 S. Atiganyanun and P. Kumnorkaew, Effects of pigment volume concentration on radiative cooling properties of acrylic-based paints with calcium carbonate and hollow silicon dioxide microparticles, *Int. J. Sustain. Energy*, 2023, **42**(1), 612–626, DOI: **10.1080/14786451.2023.2221082**.

16 N. Makaremi, E. Salleh, M. Z. Jaafar and A. H. GhaffarianHoseini, Thermal comfort conditions of shaded outdoor spaces in hot and humid climate of Malaysia, *Build. Environ.*, 2012, **48**(1), 7–14.

17 *Solcast API Toolkit* [Internet]. [cited 2023 Apr 3], available from: **https://toolkit.solcast.com.au/historical/timeseries/request**.

18 K. D. Weiss, Paint and coatings: A mature industry in transition, *Prog. Polym. Sci.*, 1997, **22**(2), 203–245.

19 *What is the difference between water-based paint and solvent-based paint?*, Normans Media Ltd, Coventry, 2022

[Internet], [cited 2023 Mar 31] available from: https://www.quora.com/What-is-the-difference-between-a-solvent-based-and-a-water-based-paint-system#:~:text=Solvent%2Dbased%20paint%20uses%20organic,resistant%20to%20wear%20and%20tear.

20 A. W. Harrison and M. R. Walton, Radiative cooling of TiO2 white paint, *Sol. Energy*, 1978, **20**(2), 185–188.

21 O. Berger, D. Inns and A. G. Aberle, Commercial white paint as back surface reflector for thin-film solar cells, *Sol. Energy Mater. Sol. Cells*, 2007, **91**(13), 1215–1221.

22 X. Berger and J. Bathiebo, Directional spectral emissivities of clear skies, *Renew. Energy*, 2003, **28**(12), 1925–1933.

23 C. Y. Tso, K. C. Chan and C. Y. H. Chao, A field investigation of passive radiative cooling under Hong Kong's climate, *Renew. Energy*, 2017, **106**, 52–61.

24 C. Liu, Y. Wu, B. Wang, C. Y. Zhao and H. Bao, Effect of atmospheric water vapor on radiative cooling performance of different surfaces, *Sol. Energy*, 2019, **183**, 218–225.

25 T. Suichi, A. Ishikawa, Y. Hayashi and K. Tsuruta, Performance limit of daytime radiative cooling in warm humid environment, *AIP Adv.*, 2018, **8**(5), 055124.

26 E. A. Goldstein, A. P. Raman and S. Fan, Sub-ambient non-evaporative fluid cooling with the sky, *Nat. Energy*, 2017, **2**(9), 1–7. Available from: https://www.nature.com/articles/nenergy2017143.

27 D. Zhao, A. Aili, Y. Zhai, J. Lu, D. Kidd, G. Tan, *et al.*, Subambient Cooling of Water: Toward Real-World Applications of Daytime Radiative Cooling, *Joule*, 2019, **3**(1), 111–123.

28 J. Liu, J. Zhang, D. Zhang, S. Jiao, J. Xing, H. Tang, *et al.*, Sub-ambient radiative cooling with wind cover, *Renew. Sustain. Energy Rev.*, 2020, **130**, 109935.

29 K. D. Dobson, G. Hodes and Y. Mastai, Thin semiconductor films for radiative cooling applications, *Sol. Energy Mater. Sol. Cells*, 2003, **80**(3), 283–296.

30 Z. Chen, L. Zhu, A. Raman and S. Fan, Radiative cooling to deep sub-freezing temperatures through a 24-h day–night cycle, *Nat. Commun.*, 2016, **7**(1), 1–5. Available from: https://www.nature.com/articles/ncomms13729.

31 M. M. Hossain and M. Gu, Radiative Cooling: Principles, Progress, and Potentials, *Adv. Sci.*, 2016, **3**(7), 1500360, DOI: 10.1002/advs.201500360.

32 Y. Weng, W. Zhang, Y. Jiang, W. Zhao and Y. Deng, Effective daytime radiative cooling via a template method based PDMS sponge emitter with synergistic thermo-optical activity, *Sol. Energy Mater. Sol. Cells*, 2021, **230**, 111205.

33 J. P. Bijarniya, J. Sarkar and P. Maiti, Review on passive daytime radiative cooling: Fundamentals, recent researches, challenges and opportunities, *Renew. Sustain. Energy Rev.*, 2020, **133**, 110263.

34 H. Tang, S. Li, Y. Zhang, Y. Na, C. Sun, D. Zhao, *et al.*, Radiative cooling performance and life-cycle assessment of a scalable MgO paint for building applications, *J. Clean. Prod.*, 2022, **380**, 135035.